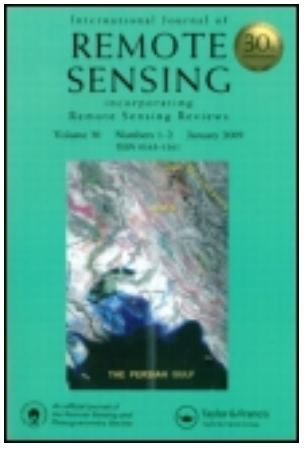

International Journal of Remote Sensing

Publication details, including instructions for authors and subscription information:
http://www.tandfonline.com/loi/tres20

Spectral unmixing of multiple lichen species and underlying substrate

Matthew Morison[a], Edward Cloutis[a] & Paul Mann[a]

[a] Department of Geography, University of Winnipeg, Winnipeg, Canada

Published online: 02 Jan 2014.

To cite this article: Matthew Morison, Edward Cloutis & Paul Mann (2014) Spectral unmixing of multiple lichen species and underlying substrate, International Journal of Remote Sensing, 35:2, 478-492

To link to this article: http://dx.doi.org/10.1080/01431161.2013.871085

International Journal of Remote Sensing, 2013
Vol. 35, No. 2, 478–492, http://dx.doi.org/10.1080/01431161.2013.871085

Taylor & Francis
Taylor & Francis Group

Spectral unmixing of multiple lichen species and underlying substrate

Matthew Morison, Edward Cloutis*, and Paul Mann

Department of Geography, University of Winnipeg, Winnipeg, Canada

(*Received 4 July 2013; accepted 24 October 2013*)

Cryptogamic covers are a wide range of photoautotrophic plants which synthesize their own food while using sunlight as an energy source. Globally, cryptogrammic covers (such as cyanobacteria, algae, fungi, lichens, and bryophytes) annually uptake about 7% of the net primary production of terrestrial vegetation and account for about half of annual biological terrestrial nitrogen fixation. On the basis of these contributions to global carbon and nitrogen cycling, it is crucial to be able to accurately monitor seasonal and regional patterns of cryptogamic cover distribution and abundance. However, lichen-encrusted rock seldom comprises 100% of the ground cover within a pixel of remote-sensed imagery, and thereby arise challenges in lichen mapping and monitoring. Here we explore spectroscopic methods and spectral mixture analysis (SMA) to overcome the challenges of reflectance spectroscopy-based optical remote sensing detection and characterization of crustose lichen species. One suite of discrete wavelengths (λ_1 = {400, 470, 520, 570, 680, 800, 1080, 1120, 1200, 1300, 1470, 1670, 1750, 2132, 2198, 2232 nm}) and two wavelength regions (λ_2 = {λ: 800 nm ≤ λ ≤ 1300 nm} and λ_3 = {λ: 2000 nm ≤ λ ≤ 2400 nm}) were investigated for their ability to discriminate between substrate and different lichen species. We found that the spectral region 800–1300 nm performed best at lichen-substrate differentiation and interspecial lichen differentiation. Furthermore, measures of central tendency from multiple wavelength regions are superior to most individual wavelength regions, particularly for lichen-rock unmixing.

1. Introduction

Lichens are a type of crypotogamic cover, consisting of a symbiotic relationship between a fungus (mycobiont) and a photosynthetic, green algae, or cyanobacteria partner referred to as a photobiont (Rees, Tutubalina, and Golubeva 2004). Globally, cryptogamic covers annually uptake around 3.9 Pg of carbon, about 7% of the net primary production of terrestrial vegetation, and around 49 Tg of nitrogen, about half of the annual biological terrestrial nitrogen fixation (Elbert et al. 2012). The geographic distribution of many lichen species make *in situ* monitoring costly and inefficient in areas such as boreal forest and tundra zones, where lichens comprise up to 70% of the terrestrial ground cover (Solheim et al. 2000), and remote areas where lichens function as the dominant terrestrial organism, such as Antarctica (Kappen 1983), European mountainous areas, and northern hemispheric continental subarctic regions (Nordberg and Allard 2002).

Hyperspectral remote-sensing systems have been identified as a desired methodology to monitor lichen extent and abundance (Zhang, Rivard, and Sánchez-Azofeifa 2005; Rees, Tutubalina, and Golubeva 2004; Feng et al. 2013). Several key requirements for remote lichen monitoring are met. Lichen transmission is <3% through the 350–2500 nm

*Corresponding author. Email: e.cloutis@uwinnipeg.ca

range, allowing for reflectance data from lichen species to be spectrally unaffected by the underlying substrate (Bechtel, Rivard, and Sánchez-Azofeifa 2002). In addition, many regions characterized by abundant lichen populations are free of other diverse vegetation (Bjerke et al. 2011), such as in the subarctic region where tree cover is very sparse and the land surface is dominated by rock and lichen coverage (Bartalev et al. 2003). Further, in areas such as continental subarctic, poor drainage conditions result in wetland cover and great proportions of the region are covered by water. However, this is overcome in this case as lichens lack water-absorbing structures, a waxy cuticle and stomata (Brodo, Sharnoff, and Sharnoff 2001). As a result, water absorption occurs over the whole vegetative body (Loppi et al. 1997). Ager and Milton (1986) determined that changes in the moisture content of the lichen do not affect the locations of their absorption bands.

However, there are challenges to the remote monitoring of lichen species. Lichen-encrusted rock seldom comprises 100% of the ground cover within a pixel (Zhang, Rivard, and Sánchez-Azofeifa 2005), and thus it is not feasible to determine lichen extent directly from imagery. SMA is an established technique which uses a linear combination of endmember spectral components to approximate the abundance of each endmember within a mixture spectrum (Somers et al. 2011; Song 2005). This study is an attempt to address the issue of monitoring the abundance and distribution of terrestrial crustose lichen coverage through hyperspectral remote sensing systems, and assess the use of SMA as a tool in this regard.

Previous research has focused on the capability of remotely sensed imagery to infer reflectance signatures of minerals on the ground by unmixing substrate and lichen reflectance spectra (Zhang, Rivard, and Sánchez-Azofeifa 2005; Rogge et al. 2009). The application of this capability to mineral exploration and geological mapping is noted, however, this approach is proverbially 'throwing the baby out with the bathwater' considering applications to lichen detection, characterization, and monitoring. In particular, the amount of carbon and nitrogen that lichens are capable of fixing from the atmosphere depends on the lichen species (Lange et al. 2004; Gavazov et al. 2010). Thus, it is important to be able to not only discriminate substrate from encrusting lichen, but also to discriminate between lichen species within a mixed pixel or spectrum.

2. Methods

2.1. *Lichen-encrusted rock samples*

Fifteen lichen-encrusted rocks were selected from several localities, including Hecla Island, Manitoba (n = 4), Pinawa, Manitoba (n = 3), Churchill, Manitoba (n = 4), Eagle Butte, Alberta (n = 1), and Contwoyto Lake, Nunavut (n = 3). These samples represent a wide range of lichen species (n = 16) and substrate compositions, including basalts, limestones, quartzites, dolostone, schist, and mafic metatuff. A summary of locality, lichen species (classified into rough groupings by colour as orange, green, black, or white/grey), and substrate composition for each sample is shown in Table 1. Ten of the 15 samples contained two endmembers, a single lichen species, and underlying substrate. Five of the 15 samples contained three or more endmembers: two or more lichen species and underlying substrate.

All samples were kept air-dried from their collection until spectral reflectance measurements were made. Spectral reflectance between wet and dry samples is reported by Rees, Tutubalina, and Golubeva (2004) to differ by less than ±5%, with dry samples exhibiting slightly higher reflectance values.

Table 1. Summary of locality, lichen species (roughly classified by colour as orange, green, black, or white/grey), and substrate composition for each sample.

Sample number	Locality	Substrate composition	Lichen species
1	Hecla Island, Manitoba	Limestone	*Placynthium nigrum* (black)
2	Contwoyto Lake, Nunavut	Basalt	*Dimelaena oriena* (orange)
3	Contwoyto Lake, Nunavut	Mafic metatuff	*Umbilicaria deusta* (black)
4	Eagle Butte, Alberta	Sandstone	*Aspicilia cincera* (white/grey)
5	Pinawa, Manitoba	Granite	*Physcia caesia* (white/grey)
6	Hecla Island, Manitoba	Limestone	*Placynthium nigrum* (black)
7	Churchill, Manitoba	Quartzite	*Melanalia stygia* (black)
8	Churchill, Manitoba	Pink dolostone	*Melanelia disjuncta* (black)
9	Churchill, Manitoba	Grey schist	*Rhizocarpon geographicum* (black)
10	Hecla Island, Manitoba	Limestone	*Placynthium nigrum* (black)
11	Churchill, Manitoba	Granite	*Caloplaca cernia* (orange), *Rinodina turfacea* (black)
12	Hecla Island, Manitoba	Limestone	*Candelaria concolor* (orange), *Placynthium nigrum* (black)
13	Contwoyto Lake, Nunavut	Granite	*Arctoparmelia centrifuga* (green), *Umbilicaria deusta* (black), *Lecanora dispersa* (white/grey)
14	Pinawa, Manitoba	Granite	*Arctoparmelia centrifuga* (green), *Placynthium asperllum* (black), *Lecanora muralis* (white/grey)
15	Pinawa, Manitoba	Granite	*Candelariella aurella* (orange) *Placynthium asperllum* (black) *Lecanora muralis* (white/grey)

2.2. *Spectral and endmember abundance data*

Reflectance spectra were collected for each endmember (each lichen species on each sample and underlying substrate for each sample), as well as for a circular area containing one or more lichen species and substrate on each sample to represent a spectral mixture.

All spectral data was acquired with an ASD FieldSpec Pro HR spectrometer, which acquires data from 350 to 2500 nm with a spectral resolution of between 2 and 7 nm, and a spectral sampling interval of 1.4 nm, which is internally resampled by the spectrometer to provide 1 nm output data. Sample spectra were measured relative to a Spectralon-calibrated reflectance standard, then corrected for minor irregularities in the absolute reflectance of the standard in the 2.0–2.5 μm region and for dark current. Spectral measurements were collected using a fibreoptic (FOV = 25.4°), employing a viewing geometry of incidence = 30° and emission = 0° with an in-house collimated 50 watt quartz tungsten halogen lamp light source at the Planetary Spectrophotometer Facility at the University of Winnipeg. Each spectral curve is an average of 500 scans of a constant field of view. This observational set-up is properly referred to as biconical-bidirectional (Schaepman-Strub et al. 2006). In the ensuing discussion we will refer to it simply as reflectance or bidirectional reflectance.

To model the situation of a mixed pixel in which spectral information from both the substrate and lichen are contributing to the pixel's spectral composition, two circular carbon black masks were constructed (radii = 6.90 and 3.50 cm) to coincide with viewing heights of 15.1 and 7.7 cm, respectively, from the spectrometer's optical fibre bundle. Each sample was covered with a circular carbon black mask such that the remaining

visible area comprised heterogeneously one or more lichen species and the underlying substrate, with the abundance of lichen coverage and substrate coverage varying by sample and mask position. Once the mask was fixed on an area, high-resolution digital photographs were taken to determine areal coverage of different lichen species and substrate by employing ImageJ software (Schneider, Rasband, and Eliceiri 2012). ImageJ was used to manually trace polygons delineating areas of lichen and substrate on each sample and calculate relative abundance of each. Bidirectional reflectance spectra as defined above (representing a remotely sensed mixed pixel) were then obtained for the identical area on each sample.

2.3. Spectral mean normalization

Spectral mean normalization is a technique used to suppress wavelength-independent differences between spectral features (Wu 2004; Zhang, Rivard, and Sánchez-Azofeifa 2005). The reflectance value at each wavelength is divided by the mean reflectance value of some set of wavelengths:

$$r'(\lambda) = \frac{r(\lambda)}{\left(\frac{\sum_{\lambda \in \lambda_j} \{r(\lambda)\}}{|\lambda_j|}\right)}, \tag{1}$$

where $r'(\lambda)$ is the mean normalized reflectance at wavelength λ, $r(\lambda)$ is the raw reflectance at wavelength λ, λ_j is a set of wavelengths forming a wavelength region for analysis (for example, $\lambda_{\text{vis}} = \{\lambda : 390\,\text{nm} \leq \lambda \leq 700\,\text{nm}\}$, representing the visible region) over the index variable j for some number of wavelength regions. $|\lambda_j|$ is the size of the set of wavelengths λ_j, for example, for λ_{vis} as defined previously, $|\lambda_{\text{vis}}| = 310$.

Spectral mean normalization reflectance values may range above 100%. For example, a mean normalized reflectance value of 150% at some wavelength λ represents a reflectance 50% greater than the mean reflectance across all wavelengths under consideration (these wavelengths under consideration are precisely the set λ_j).

2.4. Spectral mixture analysis

SMA models a mixture spectrum as a linear combination of its component spectral endmembers weighted by their abundance within a field of view, and can be inverted to determine percentage abundance of known endmembers from a mixture spectrum. The abundances are determined by minimizing the squared difference function d subject to the constraints that the abundances of all k distinct endmembers sum to one and that each endmember has non-negative abundance:

$$\mathrm{d}\left(f_1, f_2, \ldots, f_k, e(\lambda)_{\{\lambda \in \lambda_j\}}\right) = \left[\sum_{\{\lambda \in \lambda_j\}} r'_{\mathrm{m}}(\lambda) - \sum_{i=1}^{k}\left(\sum_{\{\lambda \in \lambda_j\}} r'_i(\lambda) f_i + \mathrm{e}(\lambda)\right)\right]^2, \tag{2}$$

$$f_i \geq 0, \tag{3}$$

$$\sum_{i=1}^{k} f_i = 1, \tag{4}$$

where f_i is the percentage abundance of the ith endmember, $r'_{\mathrm{m}}(\lambda)$ is the mean normalized reflectance of the mixture spectrum at wavelength λ, $r'_i(\lambda)$ is the mean normalized reflectance of the ith endmember spectrum at wavelength λ, $e(\lambda)$ is an error term as a function of wavelength, and λ_j is a set of wavelengths forming a wavelength region for analysis. The Generalized Reduced Gradient (GRG) algorithm (Lasdon et al. 1978) was employed to minimize the squared difference function d and output optimal values for percentage abundance of each endmember and error functions $e(\lambda)$.

2.5. *Selecting spectral regions* $\boldsymbol{\lambda_j}$

Zhang, Rivard, and Sánchez-Azofeifa (2005) demonstrated that a single lichen endmember is suitable for performing SMA in the wavelength region from 2000 to 2400 nm. This technique is preferable when discriminating rock from lichen cover, but an extension of this technique is required in order to differentiate between multiple lichen species in the same mixture spectrum. One set of discrete wavelengths and two wavelength regions were defined in order to highlight both intra-species spectral reflectance differences between lichens and also spectral differences between lichens and their underlying substrate. In addition, these regions and wavelength set purposely avoided water bands present at 1400 and 1900 nm, as although characteristic lichen absorption bands are unaffected by moisture content (Ager and Milton 1986), many regions dominated by lichen species, such as northern continental subarctic are dominated by wet conditions year-round (Stow et al. 2004).

We identified one suite of discrete wavelengths and two wavelength intervals as being potentially useful for lichen-substrate discrimination. The first suite of discrete wavelengths (wavelength set) is a collection of 16 distinct wavelengths selected by Rees, Tutubalina, and Golubeva (2004) in their principal components analysis of reflectance spectra of subarctic lichen species from 400 to 2400 nm. The selected wavelengths, termed 'interesting wavelengths' by the authors, in nanometers, are λ_1 = {400, 470, 520, 570, 680, 800, 1080, 1120, 1200, 1300, 1470, 1670, 1750, 2132, 2198, 2232 nm}. The first spectral region is also following up work by Rees, Tutubalina, and Golubeva (2004) and based upon their recommendation for an ideal wavelength region to discriminate between lichen species, representing the infrared spectrum below the hydroxyl absorption band at 1400 nm, where $\lambda_2 = \{\lambda$: 800 nm $\leq \lambda \leq$ 1300 nm$\}$ with a 1 nm wavelength interval (integer values) between members. We have chosen this wavelength region λ_2 to determine whether intraspecial discrimination in this region can be extended to discriminating both between species and between lichen and substrate. The second wavelength region is adapted from Zhang, Rivard, and Sánchez-Azofeifa (2005), and takes advantage of the spectral distinction between rock and lichen in the range 2000–2400 nm; $\lambda_3 = \{\lambda$: 2000 nm $\leq \lambda \leq$ 2400 nm$\}$, also with a 1 nm wavelength interval (integer values) between members.

To minimize over- or under-representation of lichen or substrate endmember spectra in any one particular wavelength region, two measures of central tendency (mean and

median values) were applied to the percentage abundances yielded from SMA in each of the three wavelength sets or regions.

3. Results & discussion

3.1. Endmember spectra

Figure 1 shows mean-normalized bidirectional reflectance spectra of all lichen species and substrate endmembers. The variability (or lack thereof) in lichen spectra (across species, across colours, and between substrate and lichen) presented here provides a preliminary understanding of which wavelength regions may perform best for spectral unmixing.

3.2. Discriminating lichen cover from substrate

Table 2 summarizes the results of SMA to determine percentage abundances from each of the three wavelength sets or regions as compared to results of percentage abundance derived from digital photography. Figure 2 displays the unmixing results for each of the three wavelength sets or regions, as well as the mean and median values of abundance for all three wavelength sets or regions. Only substrate abundance is displayed, as linear regression is invariant under linear transformations, and thus results would be identical for lichen abundance.

The wavelength set or region performing best for lichen-substrate discrimination was $\lambda_2 = \{\lambda$: 800 nm $\leq \lambda \leq$ 1300 nm$\}$ (coefficient of determination $R^2 = 0.90$) *versus* $\lambda_3 = \{\lambda$: 2000 nm $\leq \lambda \leq$ 2400 nm$\}$ ($R^2 = 0.80$). This is surprising, as λ_3 was selected to take advantage of the spectral differences between lichen cover and underlying

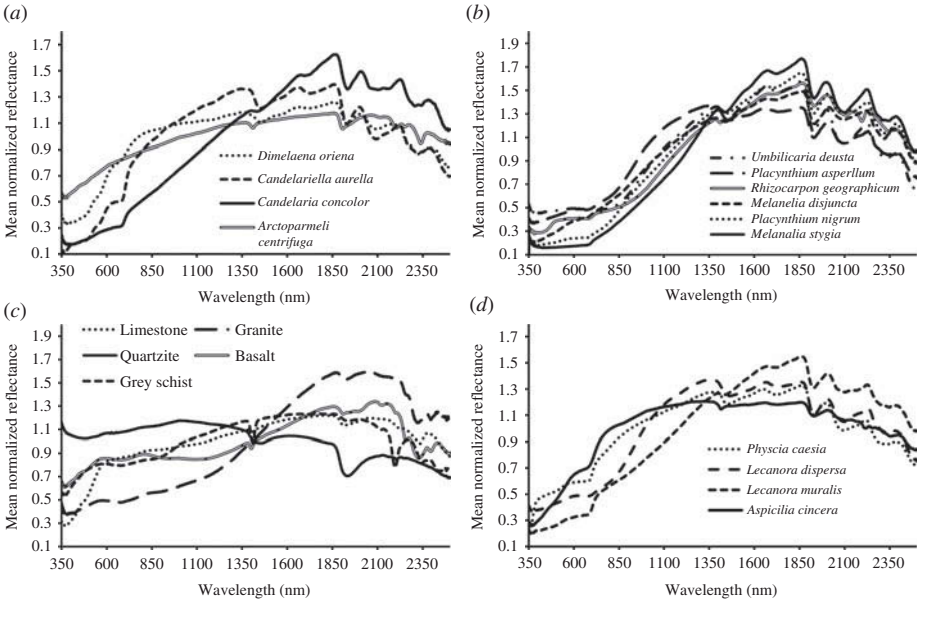

Figure 1. Normalized reflectance spectra (350–2500 nm) of endmemebers in the study: (*a*) orange and green lichen species, (*b*) black lichen species, (*c*) substrates, (*d*) white/grey species.

Table 2. Percentage abundance results of lichen cover and substrate by spectral mixture analysis (SMA) for spectral sets and regions λ_1 (λ_1 = {400, 470, 520, 570, 680, 800, 1080, 1120, 1200, 1300, 1470, 1670, 1750, 2132, 2198, 2232 nm}, λ_2 (λ_2 = {λ: 800 nm $\leq \lambda \leq$ 1300 nm}), and λ_3 (λ_3 = {λ: 2000 nm $\leq \lambda \leq$ 2400 nm}) for samples 1–10 (single lichen species and substrate mixtures).

		Abundance (%)									
Analysis method	Cover class	Sample 1	Sample 2	Sample 3	Sample 4	Sample 5	Sample 6	Sample 7	Sample 8	Sample 9	Sample 10
Digital photo	Substrate	77.1	94.5	16.6	72.9	57.3	17.9	65.8	66.6	72.3	37.3
	Lichen	22.9	5.5	83.4	27.1	42.7	82.1	34.2	33.4	27.7	62.7
SMA λ_1	Substrate	87.0	98.4	19.8	88.6	92.1	19.7	57.5	84.1	76.5	24.9
	Lichen	13.0	1.6	80.2	11.4	7.9	80.3	42.5	15.9	23.5	75.1
SMA λ_2	Substrate	79.8	98.3	20.6	73.8	81.6	27.2	78.1	84.5	78.4	32.0
	Lichen	20.2	1.7	79.4	26.2	18.4	72.8	21.9	15.5	21.6	68.0
SMA λ_3	Substrate	77.8	100.0	17.4	73.2	15.9	8.4	67.1	77.1	89.6	33.6
	Lichen	22.2	0.0	82.6	26.8	84.1	91.6	32.9	22.9	10.4	66.4
SMA mean	Substrate	81.5	98.9	19.3	78.5	63.2	18.4	67.6	81.9	81.5	30.2
	Lichen	18.5	1.1	80.7	21.5	36.8	81.6	32.4	18.1	18.5	69.8
SMA median	Substrate	79.8	98.4	19.8	73.8	81.6	19.7	67.1	84.1	78.4	32.0
	Lichen	20.2	1.6	80.2	26.2	18.4	80.3	32.9	15.9	21.6	68.0

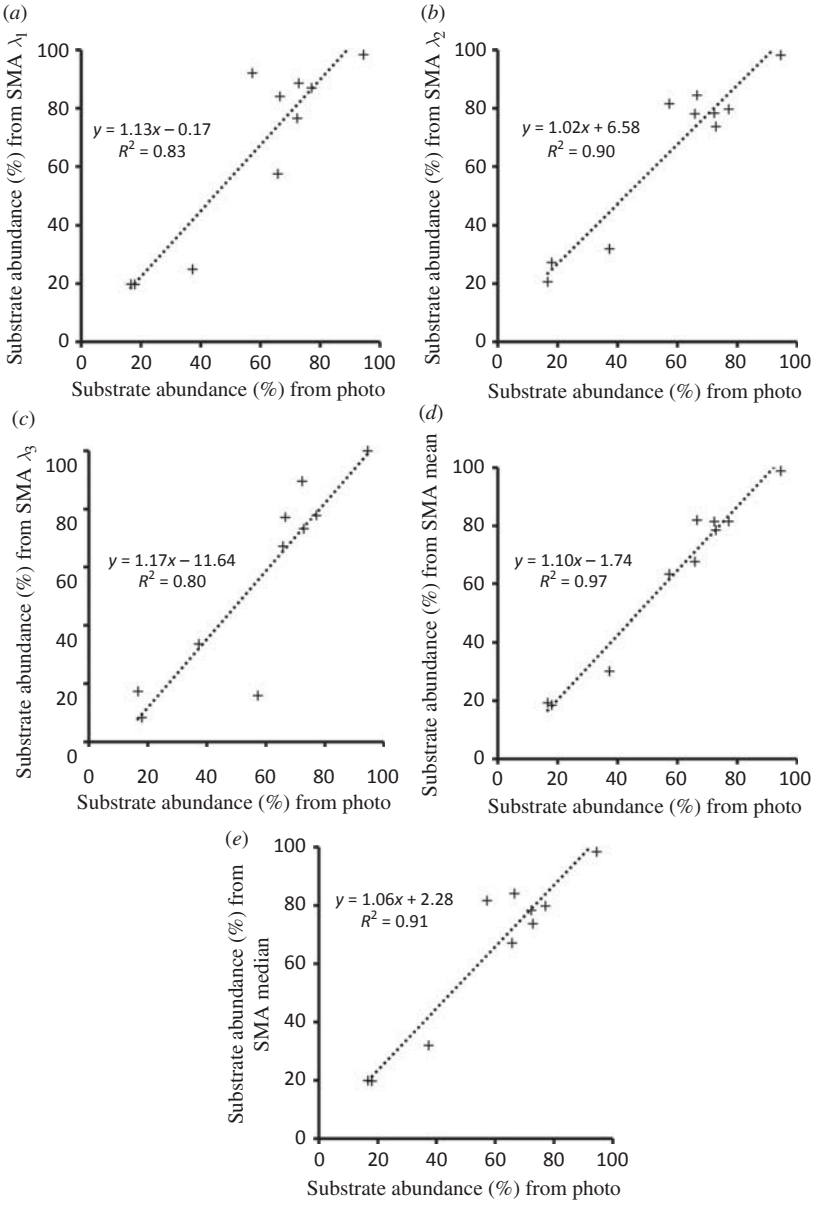

Figure 2. Results of spectral unmixing analysis to determine substrate abundance for lichen-substrate discrimination using (*a*) wavelength set λ_1, (*b*) wavelength region λ_2, (*c*) wavelength region λ_3, (*d*) mean substrate abundance values for all three wavelength sets and regions, and (*e*) median substrate abundance values for all three wavelength sets and regions.

substrate, whereas λ_2 was selected to take advantage of intra-species spectral distinctions between lichens.

For example, one sample (sample 9) where SMA λ_2 (78.4% substrate, 21.6% lichen) outperformed SMA λ_3 (89.6% substrate, 10.4% lichen) compared with the abundance from the image (72.3% substrate, 27.7% lichen). Figure 3 shows the normalized

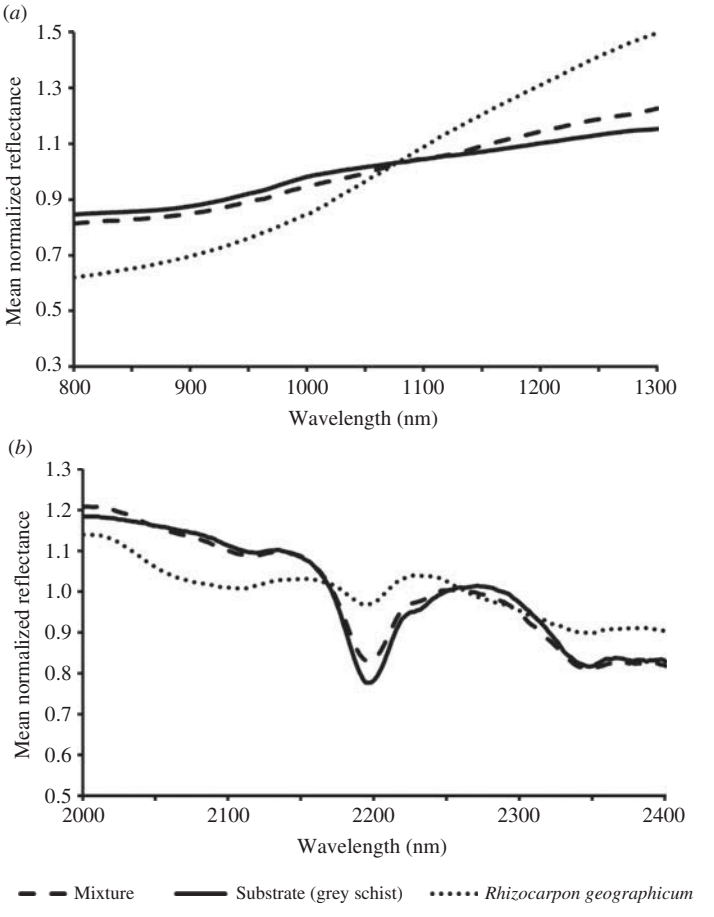

Figure 3. Normalized reflectance spectra of mixture, substrate, and lichen for sample #9 in the wavelength regions (*a*) λ_2 and (*b*) λ_3.

reflectance of the mixture as well as substrate and lichen endmembers for sample #9 (*a*) between 800 and 1300 nm (λ_2) and (*b*) between 2000 and 2400 nm (λ_3). The lichen and substrate endmembers appear, from quick examination, to be spectrally distinct in the wavelength region λ_2. Also, the mixture spectra through λ_2 appear to be an approximate linear combination of 80% of the substrate endmember spectra and 20% of the lichen endmember spectra, as was confirmed from SMA. This suggests that although the region between 800 and 1300 nm was selected to highlight spectral differences between lichen species, it appears capable of discriminating between lichen cover and substrate better than the wavelength region selected for this purpose based on the results of Zhang, Rivard, and Sánchez-Azofeifa (2005).

The mean ($R^2 = 0.97$) and median ($R^2 = 0.91$) unmixing results performed better than any of the three individual wavelength sets or regions. By capturing a wider range of variation between spectral signatures in different regions, potential over- or under-representation of any particular endmember abundance in any one wavelength region is reduced through averaging these abundance values over the three sets or regions.

Table 3. Percentage abundance results for multiple lichen species and substrate by spectral mixture analysis (SMA) for spectral sets and regions λ_1 ({400, 470, 520, 570, 680, 800, 1080, 1120, 1200, 1300, 1470, 1670, 1750, 2132, 2198, 2232 nm}, λ_2 ({λ: 800 nm $\leq \lambda \leq$ 1300 nm}), and λ_3 ({λ: 2000 nm $\leq \lambda \leq$ 2400 nm}) for samples 11–15 (multiple lichen species and substrate mixtures) in rough colour classes of species (orange, green, black, and white/grey).

		Abundance (%)				
Analysis method	Cover class	Sample 11	Sample 12	Sample 13	Sample 14	Sample 15
Digital photo	Orange species	0.6	27.4	0.0	0.0	0.8
	Green species	0.0	0.0	12.6	0.5	0.0
	Black species	41.6	12.9	15.2	12.9	2.8
	White/grey species	0.0	0.0	19.2	20.5	48.6
	Substrate	57.8	59.7	53.0	66.1	47.8
SMA λ_1	Orange species	0.0	47.1	0.0	0.0	27.9
	Green species	0.0	0.0	27.1	0.0	0.0
	Black species	0.0	0.0	11.1	14.1	5.4
	White/grey species	0.0	0.0	7.4	58.4	29.7
	Substrate	100.0	52.9	54.4	27.5	37.0
SMA λ_2	Orange species	0.0	51.2	0.0	0.0	0.0
	Green species	0.0	0.0	10.5	10.5	0.0
	Black species	0.0	0.5	0.5	10.7	11.9
	White/grey species	0.0	0.0	21.9	50.6	32.0
	Substrate	100.0	48.4	67.2	28.1	56.0
SMA λ_3	Orange species	0.0	46.6	0.0	0.0	8.4
	Green species	0.0	0.0	39.8	52.9	0.0
	Black species	0.0	0.0	1.8	0.2	0.0
	White/grey species	0.0	0.0	0.7	3.1	47.5
	Substrate	100.0	53.4	57.6	43.8	44.2
SMA mean	Orange species	0.0	48.3	0.0	0.0	12.1
	Green species	0.0	0.0	25.8	21.1	0.0
	Black species	0.0	0.2	4.5	8.3	5.8
	White/grey species	0.0	0.0	10.0	37.4	36.4
	Substrate	100.0	51.6	59.7	33.2	45.7
SMA median	Orange species	0.0	47.1	0.0	0.0	8.4
	Green species	0.0	0.0	27.1	10.5	0.0
	Black species	0.0	0.0	1.8	10.7	5.4
	White/grey species	0.0	0.0	7.4	50.6	32.0
	Substrate	100.0	52.9	57.6	28.1	44.2

3.3. *Discriminating between lichen species*

Table 3 summarizes the results of SMA to determine percentage abundances between various lichen species compared with percentage abundances derived from digital photography. Figure 4 displays the unmixing results for each of the three wavelength sets or regions, as well as the mean and median values for all three wavelength sets or regions. Abundance values from SMA and digital photography are displayed for each lichen species and substrate cover.

Similar to results for discriminating between mixtures of substrate and only one lichen species, the best wavelength set or region for discriminating between substrate and multiple lichen species was λ_2 = {λ: 800 nm $\leq \lambda \leq$ 1300 nm} (R^2 = 0.47), compared with λ_1 (R^2 = 0.36) or λ_3 (R^2 = 0.41). This is not surprising as λ_2 was selected for interspecies discrimination as described by Rees, Tutubalina, and Golubeva (2004).

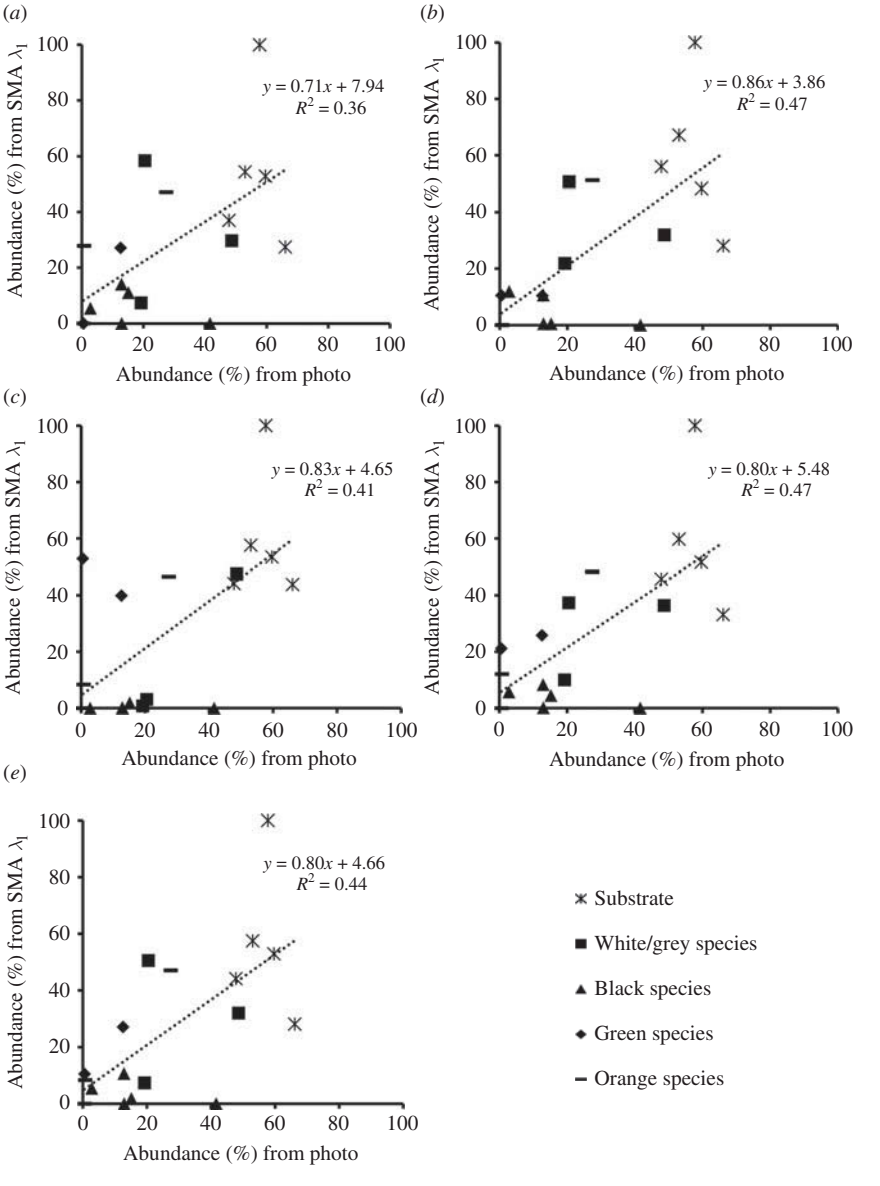

Figure 4. Results of spectral unmixing analysis to determine abundance of multiple lichen species and substrate using (*a*) wavelength set λ_1, (*b*) wavelength region λ_2, (*c*) wavelength region λ_3, (*d*) mean abundance values for all three wavelength sets and regions, and (*e*) median abundance values for all three wavelength sets and regions.

For example, spectral unmixing of sample 13 was more successful (although still not to an ideal standard) at interspecies lichen discrimination compared with digital photography (12.6% green lichen species, 15.2% black lichen species, 19.2% grey lichen species, 53.0% substrate) in the wavelength region λ_2 (27.1% green lichen species, 11.1% black lichen species, 7.4% grey lichen species, 67.2% substrate) than for the wavelength region λ_3 (39.8% green lichen species, 1.8% black lichen species, 0.7%

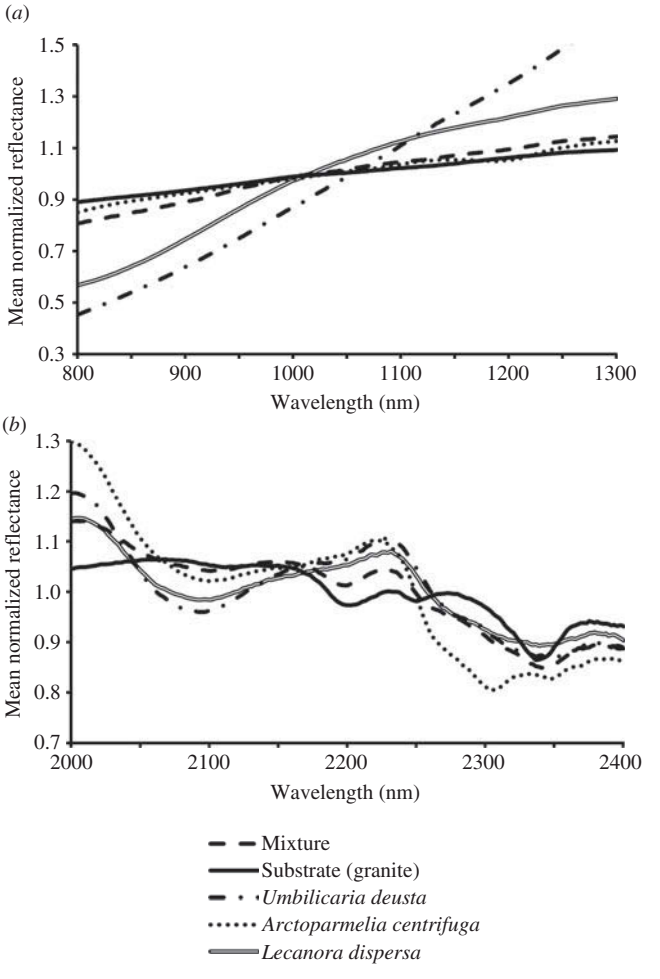

Figure 5. Normalized reflectance spectra of mixture, substrate, and lichen for sample #13 in the wavelength regions (*a*) λ_2 and (*b*) λ_3.

grey lichen species, 57.6% substrate). Figure 5 displays normalized reflectance spectra for each lichen endmember, the substrate endmember, and the mixture spectra. These results confirm the work of Rees, Tutubalina, and Golubeva (2004), who suggested that lichen species may be spectrally differentiated in the region between 800 and 1300 nm. In this case, λ_3 performed better than λ_2 at discriminating between total lichen coverage (all species) and substrate, consistent with previous work by Zhang, Rivard, and Sánchez-Azofeifa (2005) that the wavelength region between 2000 and 2400 is optimal for distinguishing between lichen spectra (independent of species) and substrate. This suggests that when not concerned with lichen species composition but faced with the challenge of multiple lichen species, spectral unmixing in the 2000 to 2400 nm region is preferred.

The mean (R^2 = 0.47) and median (R^2 = 0.44) unmixing results performed better than unmixing for the λ_1 wavelength set and λ_3 wavelength region; however, in this case, both measures of central tendency performed equally well or worse than unmixing results from the λ_2 region.

In all cases, R^2 values for unmixing results were much lower for multiple lichen species (ranging from 0.36 to 0.47) than single lichen species and substrate mixtures (0.80 to 0.97). The complexity of three or four endmembers in an unmixing model makes the problem much more difficult, particularly when multiple endmembers are spectrally ambiguous (as is the case with many lichen species in the selected wavelength set or regions), illustrated in the case of sample #13 in Figure 4.

Of note is the fact that in this study all lichen species under consideration were of crustose type. Many environments investigated for lichen abundance and coverage through hyperspectral remote sensing systems may be covered (predominantly or peripherally) by other lichen morphologies (foliose and fruiticose). These other morphologies may have spectral properties that were not accounted for in this work and deserving of similar treatment to determine whether spectral unmixing is a feasible method to discriminate lichen cover intramorphologically, and between fruiticose and foliose lichens and substrate.

4. Conclusions

This study has assessed the potential to employ SMA to determine abundance of substrate and one or more lichen species within a mixture. One wavelength set and two wavelength regions (λ_1 = {400, 470, 520, 570, 680, 800, 1080, 1120, 1200, 1300, 1470, 1670, 1750, 2132, 2198, 2232 nm}, λ_2 = {λ: 800 nm $\leq \lambda \leq$ 1300 nm}, and λ_3 = {λ: 2000 nm $\leq \lambda \leq$ 2400 nm}) were investigated for their ability to discriminate between substrate and different lichen species. Water absorption bands at 1400 and 1900 nm were purposefully avoided in each wavelength set or region.

The mean and median unmixing results performed better than unmixing in the λ_1 set and λ_3 region; however, in this case, both measures of central tendency performed equally well or worse than unmixing results from the λ_2 region. In all cases, R^2 values for unmixing results were much lower for multiple lichen species (ranging from 0.36 to 0.47) than single lichen species and substrate mixtures (0.80 to 0.97). The complexity of three or four endmembers in an unmixing model makes the problem much more difficult, particularly when multiple endmembers are spectrally ambiguous (as is the case with many lichen species in the selected wavelength set and regions).

In both cases of lichen-substrate differentiation and interspecial lichen differentiation, the wavelength region between 800 and 1300 nm performed better than the region between 2000 and 2400 nm and the wavelength set consisting of the wavelengths λ_1 = {400, 470, 520, 570, 680, 800, 1080, 1120, 1200, 1300, 1470, 1670, 1750, 2132, 2198, 2232 nm}. However, when considering the challenge of lithological mapping in areas of multiple lichen species, unmixing in the spectral region from 2000 to 2400 nm performed best for determining total lichen abundance (species-independent) and substrate abundance. The mean and median abundance value from SMA of several different wavelength sets or regions performed better than the SMA in any individual wavelength set or region.

Previous studies employing SMA to unmix lichen and substrate have focused on the application of this procedure for lithologic mapping using published spectra of rock encrusting lichens, combined with the usage of normalization procedures in different spectral regions applied to both image and endmember spectra. In doing so, some methodologies 'provide geologists with an opportunity to group all lichens into one endmember' (Zhang, Rivard, and Sánchez-Azofeifa 2005). Although effective for geological mapping, recent emphasis on the importance of lichens in global carbon and

nitrogen cycling underscores the importance of long-term lichen detection, characterization, and monitoring. In the future, a closer examination of lichen/substrate unmixing in the visible region may provide a solution to the difficulties inherent in intraspecies (or intramorphological) discrimination.

Acknowledgements

The authors also wish to thank the Canada Foundation for Innovation, the Manitoba Research Innovations Fund, the Canadian Space Agency, and the University of Winnipeg for supporting the establishment of the Planetary Spectrophotometer Facility where this work was conducted. Additional thanks are extended to G. Bedard, J. McCorquedale, R. St J. Lambert, and M. Zalick for assistance with sample collection; to M. Bennett for assistance with figure preparation; and to J. Marsh at the University of Alberta for assistance with identification of lichen species.

Funding

This research was funded by the Natural Sciences and Engineering Research Council of Canada, The Canadian Space Agency, and the University of Winnipeg.

References

Ager, C. M., and N. M. Milton. 1986. "Spectral Reflectance of Lichens and Their Effects on Reflectance of Rock Substrates." *Geophysics* 52: 898–906.

Bartalev, S. A., A. S. Belward, D. V. Erchov, and A. S. Isaev. 2003. "A New SPOT4-VEGETATION Derived Land Cover Map of Northern Eurasia." *International Journal of Remote Sensing* 24: 1977–1982.

Bechtel, R., B. Rivard, and A. Sánchez-Azofeifa. 2002. "Spectral Properties of Foliose and Crustose Lichens Based on Laboratory Experiments." *Remote Sensing of Environment* 82: 389–396.

Bjerke, J. W., S. Bokhorst, M. Zielke, T. V. Callaghan, F. W. Bowles, and G. K. Pheonix. 2011. "Contrasting Sensitivity to Extreme Winter Warming Events of Dominant Sub-Arctic Heathland Bryophyte and Lichen Species." *Journal of Ecology* 99: 1481–1488.

Brodo, I. M., S. D. Sharnoff, and S. Sharnoff. 2001. *Lichens of North America*. New Haven, CT: Yale University Press.

Elbert, W., B. Weber, S. Borrows, J. Steinkamp, B. Büdel, M. O. Andreae, and U. Pöschl. 2012. "Contribution of Cryptogamic Covers to the Global Cycles of Carbon and Nitrogen." *Nature Geoscience* 5: 459–462. doi:10.1038/ngeo1486.

Feng, J., B. Rivard, D. Rogge, and A. Sánchez-Azofeifa. 2013. "The Longwave Infrared (3–14 Mm) Spectral Properties of Rock Encrusting Lichens Based on Laboratory Spectra and Airborne SEBASS Imagery." *Remote Sensing of Environment* 131: 173–181. doi:10.1016/j.rse.2012.12.018.

Gavazov, K. S., N. A. Soudzilovskaia, R. S. P. van Logtestijn, M. Braster, and J. H. C. Cornelissen. 2010. "Isotopic Analysis of Cyanobacterial Nitrogen Fixation Associated with Subarctic Lichen and Bryophyte Species." *Plant and Soil* 333 (1–2): 507–517.

Kappen, L. 1983. "Ecology and Physiology of the Antarctic Lichen *Usnea Sulphurea* (Koenig) Th. Fries." *Polar Biology* 1: 249–255.

Lange, O. L., B. Büdel, A. Meyer, H. Zellner, and G. Zotz. 2004. "Lichen Carbon Gain Under Tropical Conditions: Water Relations and CO2 Exchange of Lobariaceae Species of a Lower Montane Rainforest in Panama." *The Lichenologist* 36: 1–14. doi:10.1017/S0024282904014392.

Lasdon, L. S., A. D. Waren, A. Jain, and M. Ratner. 1978. "Design and Testing of a Generalized Reduced Gradient Code for Nonlinear Programming." *ACM Transactions on Mathematical Software* 4 (1): 34–50.

Loppi, S., L. Nelli, S. Ancora, and R. Bargagli. 1997. "Accumulation of Trace Elements in the Peripheral and Central Parts of a Foliose Lichen Thallus." *The Bryologist* 100: 251–253.

Nordberg, M.-L., and A. Allard. 2002. "A Remote Sensing Methodology for Monitoring Lichen Cover." *Canadian Journal of Remote Sensing* 28 (2): 262–274. doi:10.5589/m02-026.

Rees, W. G., O. V. Tutubalina, and E. I. Golubeva. 2004. "Reflectance Spectra of Subarctic Lichens Between 400 and 2400 nm." *Remote Sensing of Environment* 90: 281–292.

Rogge, D. M., B. Rivard, J. Harris, and J. Zhang. 2009. "Application of Hyperspectral Data for Remote Predictive Mapping, Baffin Island, Canada." *Reviews in Economic Geology* 16: 209–222.

Schaepman-Strub, G., M. E. Schaepman, T. H. Painter, S. Dangel, and J. V. Martonchik. 2006. "Reflectance Quantities in Optical Remote Sensing – Definitions and Case Studies." *Remote Sensing of Environment* 103: 27–42.

Schneider, C. A., W. S. Rasband, and K. W. Eliceiri. 2012. "NIH Image to ImageJ: 25 Years of Image Analysis." *Nature Methods* 9: 671–675.

Solheim, I., O. Engelsen, B. Hosgood, and G. Andreoli. 2000. "Measurement and Modeling of the Spectral and Directional Reflection Properties of Lichen and Moss Canopies." *Remote Sensing of Environment* 72: 78–94.

Somers, B., G. P. Asner, L. Tits, and P. Coppin. 2011. "Endmember Variability in Spectral Mixture Analysis: A Review." *Remote Sensing of Environment* 115: 1603–1616.

Song, C. H. 2005. "Spectral Mixture Analysis for Subpixel Vegetation Fractions in the Urban Environment: How to Incorporate Endmember Variability?" *Remote Sensing of Environment* 95: 248–263.

Stow, D. A., A. Hope, D. McGuire, D. Verbyla, J. Gamon, F. Huemmrich, S. Houston, C. Racine, M. Sturm, K. Tape, L. Hinzman, K. Yoshikawa, C. Tweedie, B. Noyle, C. Silapaswan, D. Douglas, B. Griffith, G. Jia, H. Epstein, D. Walker, S. Daeschner, A. Petersen, L. Zhou, and R. Myneni. 2004. "Remote Sensing of Vegetation and Land-Cover Change in Arctic Tundra Ecosystems." *Remote Sensing of Environment* 89: 281–308.

Wu, C. 2004. "Normalized Spectral Mixture Analysis for Monitoring Urban Composition Using ETM+ Imagery." *Remote Sensing of Environment* 93: 480–492.

Zhang, J., B. Rivard, and A. Sánchez-Azofeifa. 2005. "Spectral Unmixing of Normalized Reflectance Data for the Deconvolution of Lichen and Rock Mixtures." *Remote Sensing of Environment* 95 (1): 57–66. doi:10.1016/j.rse.2004.11.019.